



SYNTHESIS AND CHARACTERIZATION OF CDS QUANTUM DOTS COATED WITH METHOTREXATE FOR TARGETED DRUG DELIVERY AGAINST CANCER TREATMENT

Amber Mubeen¹, Asma Irshad², Ansar Zubair³, Tahira Batool⁴ and Faqeeha Javed⁵

¹Department of Biotechnology, University of Okara, Okara

²School of Biochemistry and Biotechnology, University of the Punjab, Lahore, Pakistan

³Department of Zoology, University of Education, Lahore, Pakistan

⁴Allied health sciences, Superior University, Lahore, Pakistan

⁵Riphah International University, Gulberg campus, Lahore

***Corresponding Author:** Dr. Asma Irshad (PhD Biochemistry)

*School of Biochemistry and Biotechnology, University of the Punjab, Lahore-Pakistan, Phone: +92 323 8403178, Email: asmairshad76@yahoo.com

ABSTRACT

Cancer is the second leading cause of health-related issues, contributing significantly to the high mortality rate. Methotrexate (MTX), a potent anticancer drug derived from folic acid, is widely used to treat various cancers. However, its application is often limited by the ability of cancer cells to develop resistance. By conjugating MTX with quantum dots (QDs) to form nanoconjugates (NCs), the drug can be more effectively taken up by cells through folate receptor (FR)-mediated endocytosis minimizing off-target effects enabling precise anticancer drug delivery to tumor sites. In the current study, we synthesized MTX-conjugated cysteine-capped CdS QDs (MTX-QD Nanocomposites) and evaluated their cytotoxicity on MCF-7 cells. CdS QDs were prepared through a chemical wet method under high temperature and pressure, followed by conjugation with MTX using a glutaraldehyde method. The synthesis of QDs were confirmed by light microscopy emitted yellowish green fluorescence. The characterization of CdS QDs and their conjugation with cysteine, folic acid, and MTX was confirmed by UV-Vis spectra at 520-530 nm. The MTX-QD Nanocomposites were characterized by FT-IR, SEM and XRD. Based on FT-IR spectra, the functional groups associated with MTX-QD Nanocomposites were determined. SEM analysis revealed that the general surface of MTX-CdS QDs was in tightly packed confirmation and free from agglomeration. XRD spectra showed diffraction peaks at 2θ values 32.92° , 47.19° , 55.89° , 58.71° , and 68.45° in pattern. The binding efficiency of folic acid-conjugated MTX-CdS QD nanocomposites to folate receptors in cancer tissues was confirm through immunohistochemistry. Anticancer activity was assessed through MTT Assay. The MTT assay demonstrated that these Nanocomposites significantly reduced cell viability in a concentration-dependent manner. ELISA microplate reader analysis confirmed that cell viability decreased to 21.87% at a 500 ng/mL concentration of MTX-QD Nanocomposites, indicating a high rate of cell death. The viability of MCF-7 cells exposed to MTX-CdS QD nanocomposites using the MTT cell viability assay compared to the control. Results indicate that increasing concentrations of MTX-CdS QDs lead to a significant decrease in cell viability.

Keywords: MTX; CdS QDs; UV-Vis; XRD; FT-IR; SEM; MTT Assay; immunohistochemistry; MCF-7 cells

INTRODUCTION

Cancer is a complex, multifactorial disease resulting from the interaction between environmental factors and genetic predispositions, and it is the second leading cause of death worldwide (Raj et al., 2021; Klochkov et al., 2021). The unchecked proliferation of cells leads to cancer, transforming normal cells into malignant ones during the replacement of old cells (Bonacci & Emanuele, 2020). Statistically, one in six women and one in five men will develop cancer in their lifetime. In Pakistan, approximately 150,000 new cancer cases are reported annually, with a mortality rate of 60% to 80% (Shamsi, 2020). Globally, cancer is responsible for over 8 million deaths each year, and the number of new cases continues to rise, underscoring the need for effective and safe treatments (Sheth et al., 2020).

Treating cancer is particularly challenging due to the ability of cancer cells to develop resistance to anticancer drugs, sustain proliferative signaling, metastasize, evade growth suppressors, and induce angiogenesis (Kumari et al., 2021). Traditional chemotherapy, once the primary treatment choice, faces several pharmaceutical limitations, including drug-drug interactions, stability issues, drug resistance, and poor aqueous solubility (Hassan et al., 2021). Currently, four major treatment approaches are used in clinical settings: cytoreductive surgery, chemotherapy, radiation therapy, and immunotherapy (Sheth et al., 2020). While these strategies have improved survival rates and treatment efficacy, they also have significant drawbacks, such as the cytotoxicity to healthy cells and numerous unwanted side effects (Kumari et al., 2021).

Conventional therapies suffer from nonspecific drug delivery, largely due to physical and enzymatic barriers that prevent drugs from reaching their targeted sites effectively (Hassan et al., 2021). Nanotechnology has revolutionized cancer treatment by offering new possibilities for safe and effective therapies (Hassan et al., 2021). In recent years, nanomedicine has emerged as a key application of nanotechnology, aiming to balance drug effectiveness and toxicity by controlling the accumulation and biodistribution of chemotherapeutic agents (Cabral et al., 2024). Despite advancements, the heterogeneity and diversity of cancer cells make it difficult to develop personalized anticancer therapies. DNA/RNA-based drugs, which offer more personalized and safer treatment options, are promising. Nanocarriers for DNA/RNA delivery present a promising research area for targeting cancer cells effectively (Davodabadi., 2014). Nanotechnology operates at the nanoscale, controlling the reconstruction of matter at atomic and molecular levels within a size range of 1 to 100 nm. Nanoparticles, the building blocks of nanotechnology, have significant applications in medicine due to their size-dependent chemical and physical characteristics, which align with most biological structures and molecules (Malik & Muhammad, 2023). This makes nanoparticles ideal for *in vivo* and *in vitro* biomedical applications, including imaging, targeted drug delivery, biosensing, and artificial implants (Majeed & Qaddoori, 2023).

Nanotechnology-based chemotherapy has opened new avenues for cancer treatment (Hassan et al., 2021). Nanotechnology-based drug delivery systems enable the targeted transport of macromolecules and micromolecules, enhancing the bioavailability of drugs to target cells by penetrating tissues and crossing epithelial surfaces effectively (Hassan et al., 2021). Nanoparticles can be classified into organic, inorganic, and carbon-based groups, each with unique properties and applications (Irshad et al., 2020; Osama et al., 2020).

Quantum dots (QDs) are a remarkable group of inorganic nanoparticles used in various biomedical and industrial applications. Their size, ranging from 2 to 10 nm, allows for unique optoelectronic properties that make them highly resistant to chemical degradation and photobleaching (Phafat & Bhattacharya, 2023). QDs are particularly valuable in medical fields for real-time tissue imaging, cancer biomarker detection, diagnostics, single-molecule probes, and drug delivery (Omidian et al., 2024). Current diagnostic techniques, such as tissue biopsy, medical imaging, and biomarker detection, are often insufficiently sensitive, time-consuming, labor-intensive, and costly. In contrast, QD-based detection offers a faster, easier, and more economical solution, allowing quick point-of-care cancer marker screening (Singh et al., 2020; Iannazzo et al., 2021). QDs, used in techniques like fluorescence-linked immunosorbent assay (FLISA), provide powerful and stable fluorescence,

resistance to photobleaching, and extremely sensitive detection capabilities (Alaghmandfard et al., 2021).

MATERIALS AND METHODS

Synthesis of Cadmium Sulfide Quantum Dots Using Chemical Method

A 200 mL beaker was cleaned and filled with 100 mL of 0.01 M cadmium acetate, boiled at 150°C. The pH was adjusted to 10 using 1 M NaOH, then 100 mL of 0.01 M sodium sulfide was added. The solution was mixed, covered with aluminum foil, and placed inside a 500 mL beaker half-filled with water. This was then placed inside a 1000 mL beaker half-filled with water, all covered with aluminum foil. The setup was heated on a hot plate with stirring between 120°C and 150°C for 15 hours.

Preparation of Quantum Dots Conjugated with Cysteine

The sample was centrifuged at 10,000 rpm for 20 minutes to form a pellet, which was washed with distilled water and recentrifuged. The pellet was solubilized in 50 mL distilled water, and 20 mL of 0.01 M cysteine was added. The sample was incubated at 100°C for 5 hours, then recentrifuged at 10,000 rpm for 20 minutes. The supernatant was frozen and thawed to settle particles, dried at 45°C overnight, and analyzed spectrophotometrically. The ninhydrin test confirmed cysteine binding to CdS QDs.

Conjugation of Folic Acid to Cysteine-Capped CdS QDs

In a 50 mL falcon tube, 10 mg of cysteine-capped CdS QDs were mixed with 25 mL of 0.01 M pyridine coupling buffer for 10 minutes. Glutaraldehyde was added to a final concentration of 5%, and the mixture was incubated at room temperature with shaking at 100 rpm for 3 hours. Then, 5 mg of folic acid was added and incubated for 24 hours with shaking. The solution was centrifuged at 7,000 rpm for 10 minutes, the supernatant discarded, and 1 mL of 1 M glycine was added to the pellet and incubated for 30 minutes. The sample was recentrifuged, washed with wash buffer, and recentrifuged again. The pellet was stored in PBS at 4°C and analyzed with FTIR.

Synthesis of Methotrexate-Conjugated CdS-Cys-Folic Acid Particles

Cys-CdS particles conjugated with folic acid were washed with wash buffer and mixed with 25 mL of 0.01 M pyridine coupling buffer for 10 minutes. Glutaraldehyde was added to 5%, and the mixture was incubated for 3 hours with shaking at 100 rpm. After 3 hours, 100 mg of methotrexate was added and incubated for 24 hours with shaking. The solution was centrifuged at 7,000 rpm for 10 minutes, the supernatant discarded, and 1 mL of 1 M glycine was added to the pellet and incubated for 30 minutes. The sample was recentrifuged, washed with wash buffer, and recentrifuged again. The pellet was stored in PBS at 4°C and analyzed with FTIR.

Applied Nanoscience

Characterization of MTX-conjugated cysteine-capped CdS QDs

The samples MTX-CdS QDs nanoparticles were characterized by the following techniques.

Compound Microscopy Compound microscopy was used to examine Cys-CdS quantum dots using objective lenses with magnifications of 10X and 100X. A clean glass slide was prepared, and a few drops of Cys-CdS quantum dots were dispensed onto it from a Falcon tube. The slide was then observed under white light with a wavelength range centered around 520 nm (Wang et al., 2021).

Ultraviolet visible spectroscopy Ultraviolet-visible (UV-Vis) spectroscopic analysis was performed using a UV-Vis spectrometer. Sample solutions of CdS QDs were prepared with distilled water. The UV-Vis measurements were taken within the wavelength range of 480 to 540 nm, and the spectra of the samples were recorded within the specified wavelength range of mentioned above (Alsaggaf et al., 2020).

Fourier transformation infrared spectroscopy (FT-IR) The FT-IR was conducted on MTX-conjugated cysteine-capped CdS QDs to identify their functional groups. The infrared spectra were obtained using a Fourier transform infrared spectrometer at room temperature in dry air. To prepare the samples for FT-IR spectroscopy, potassium bromide (KBr) pellets were employed. These KBr pellets facilitated the determination of the Fourier transform infrared spectra using the FT-IR spectrophotometer (Irshad et al., 2020).

Scanning electron microscopy-energy dispersion spectroscopy SEM analysis was conducted to examine the surface morphology and structural modifications within a structure and to confirm the different bonding concomitant with of MTX-CdS QDs nanoparticles at a magnification of 2000X (Kadam et al., 2021).

X-ray diffraction (XRD) analysis X-ray diffraction (XRD) was utilized to assess the phase purity of the prepared products MTX-CdS QDs nanoparticles. This technique enabled the determination of the crystalline phases present in the samples, confirming their structural integrity and composition., and the structure was discovered to be in a monoclinic system (Ganguly & Nath, 2020).

Confirmation Test to Check the In-Vitro Anticancer Activity of MTX- CdSQD Nanocomposites on MCF-7 cells

Anticancer activity of MTX-CdS QDs nanocomposites was checked by performing tissue immunohistochemistry and MTT assay.

Tissue immunohistochemistry

Tissue immunohistochemistry was performed to confirm the binding of MTX-CdS QDs with cancer cell. Albumin solution was prepared, slides were coated with the solution, and dried at 50°C overnight. Cancer tissue was fixed, dehydrated using sucrose solutions, embedded in OCT compound, and frozen at -20°C. Frozen tissue blocks were trimmed, cut into thin sections using a cryostat, transferred onto albumin-coated slides, and stored at -20°C. BSA blocking was performed, followed by incubation with MTX-CdSQD nanocomposites and visualization using a fluorescent microscope.

MTT Cell Viability Assay

MTT assay was performed to evaluate the anticancer activity of MTX-CdS QD nanocomposites on MCF-7 cells. Cells were seeded in a 96-well plate and treated with different concentrations of the nanocomposites. After 72 hours of incubation, MTT reagent was added, and formazan crystals were dissolved using DMSO. The absorbance at 570nm was measured using an ELISA microplate reader. Cell viability was calculated using the following formula.

$$\text{Percentage Viability} = \frac{\text{Absorbance of Test well}}{\text{Absorbance of Control well}} \times 100$$

RESULT AND DISCUSSIONS

The synthesis of CdS QDs was performed through chemical wet method under high temperature and pressure and MTX-QD nanocomposites was prepared by using glutaraldehyde method. Confirmation of CdS QDs done under light microscope. Characterization was done by using UV-Vis spectroscopy and FTIR spectroscopy. And anticancer activity of MTX-QD nanocomposites was check on MCF-7 cells through immunohistochemistry and MTT assay. Results are given below:

Synthesis of Cysteine Capped Cadmium Sulfide Quantum Dots

The Cys-CdS QDs were synthesise by the chemical reaction between cadmium acetate and sodium sulphide to form solid cadmium sulfide and sodium acetate and yellow color was observed. When CdS QDs bind with cysteine under high temperature and pressure the change in color was observed from yellow to orange. The fine particles of CdS were collected in the form of precipitation at the bottom of the beaker



Fig.1 Synthesis of Cysteine Capped Cadmium Sulfide Quantum Dots (A) and (B) CdS QDs synthesis by using chemical method in beaker by using hot plate (C) Cadmium sulfide quantum dots at the bottom of beaker

Ninhydrin Test to Confirm Cysteine Binding to Cadmium Sulfide

The ninhydrin test was done for the confirmation of cysteine binding with CdS QDs. Appearance of violet color confirm the binding of cysteine with CdS QDs sample. The violet color indicated the presence of amino acid in CdS QDs sample while in control tube transparent color illustrate the absence of amino acid.



Fig.2 Ninhydrin test to check the binding of cysteine with CdS QD

Microscopic Analysis of CdS QDs

The CdS QDs were observed in light microscope under white light of approximately 520nm with 10X objective lens. A yellowish green fluorescence was emitted which confirm the synthesis of QDs (Figure 3).

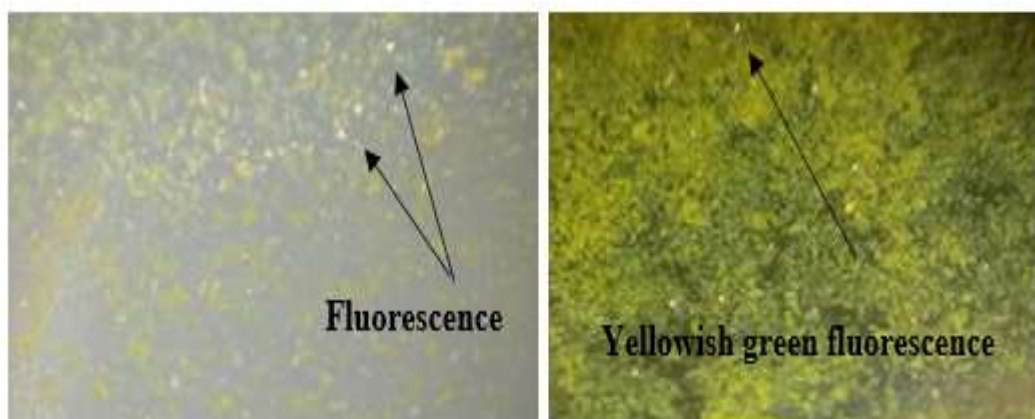


Fig. 3 CdS QDs in white light under light microscope

Characterization of MTX-Conjugated Cysteine Capped CdS QD

Characterization of MTX-CdS QDs was done by UV-Vis spectrophotometer and FTIR with following results.

UV-Vis Spectrophotometric Analysis

UV-Vis Spectrophotometric Analysis of CdS QDs Conjugated with Cysteine Spectrophotometric analysis of CdS QDs was performed under UV-Vis spectrophotometer at the range of wavelengths to obtain the absorption spectra to find out the wavelength at which the CdS QDs emit fluorescence. Table 1 shows the increment in absorbance at the wavelength of 520nm specify that the QDs glow at 520nm. Figure 4 shows a graphical explanation of CdS QDs excitation at 520 nm wavelength.

Wavelength (nm)	Absorbance
480	0.178
490	0.174
500	0.189
510	0.181
520	0.194
530	0.188
540	0.166

Table. 1 Increase in absorbance at 520nm indicates that the quantum dots give fluorescence at 520nm

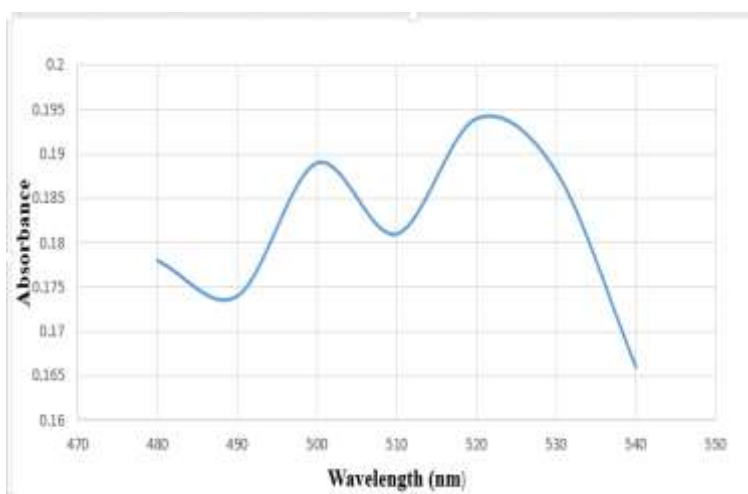


Figure. 4 Graphical explanation of CdS QDs excitation

UV-Vis Spectrophotometric Analysis of CdS Particles Conjugated with Methotrexate

The increment in absorbance at the wavelength and maximum absorption at 530nm and Figure 5 shows a graphical explanation indicates the conjugation of methotrexate with CdS QDs

Wavelength (nm)	Absorbance
480	0.179
490	0.178
500	0.174
510	0.189
520	0.181
530	0.194
540	0.188
550	0.166

Table. 2 Increase in absorbance at 540 nm indicates the conjugation of methotrexate with CdS QDs

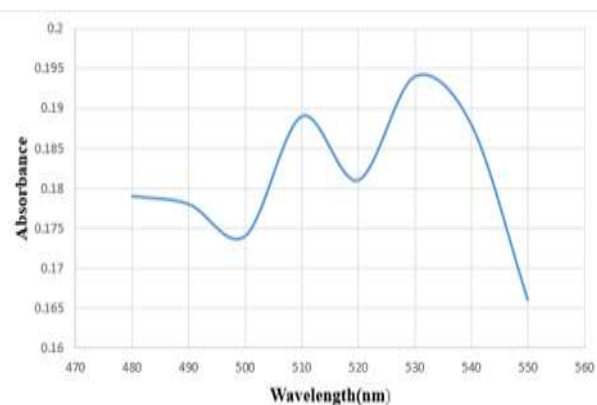


Figure. 5 Graphical interpretation of absorption spectra of Cys-CdS QDs conjugated with Methotrexate

FTIR Analysis of MTX- CdS QD Nanocomposites

FTIR Analysis of CdS-Cysteine

In FTIR analysis of CdS-Cysteine there are three distinct peaks representing the presence of C-H bond of cysteine at 3500 cm^{-1} , C=O bond peak at 1400 cm^{-1} and C-C bond peak at 1000 cm^{-1} . It specifies the binding of cysteine to CdS QDs (Figure 6).

FTIR Analysis of CdS-Cysteine-Folic acid

In FTIR analysis of CdS-Cysteine-Folic acid there are two distinct peaks illustrating the presence of two compounds with C-H stretch at around $3600\text{--}3700\text{ cm}^{-1}$ while several other peaks show the presence of C=O, C=C, C-N bonds in folic acid at $1500\text{ to }1000\text{ cm}^{-1}$ confirm the binding of folic acid with the composite (Figure 7).

FTIR Analysis of CdS-Cysteine-Folic acid-Methotrexate

In FTIR analysis of CdS-Cysteine-Folic acid-Methotrexate illustrate peaks at $1500\text{--}1000\text{ cm}^{-1}$ increase as methotrexate has many C=C, C-N and C=O bonds. While peaks around 3500 cm^{-1} shows N-H, O-H and C-H bonding in methotrexate. It confirms the binding of methotrexate to Cys- CdS QDs composite (Figure 8).

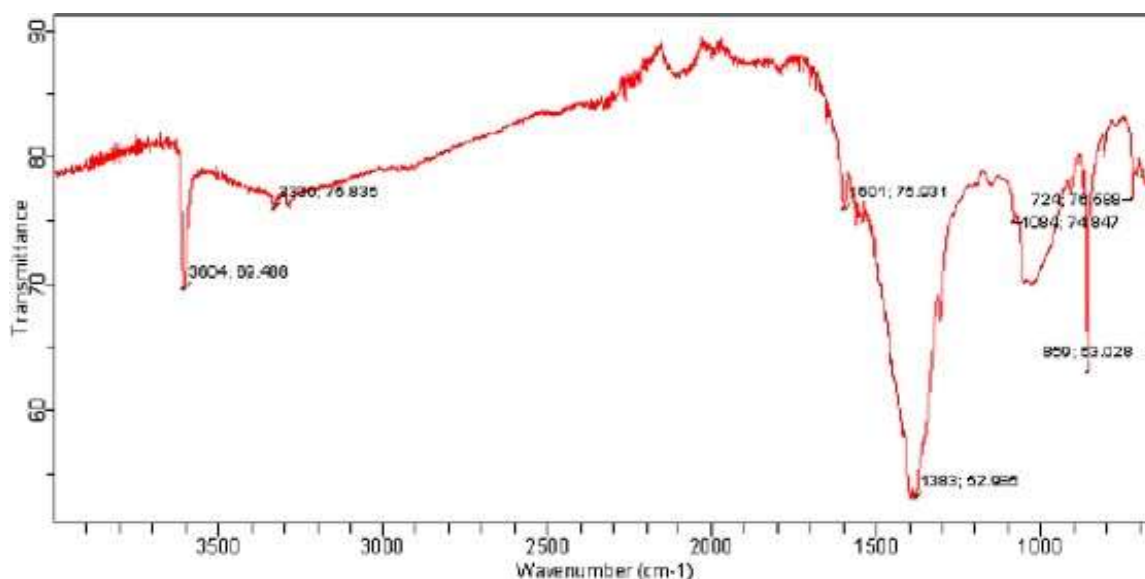


Fig. 6 FTIR analysis of CdS- Cysteine

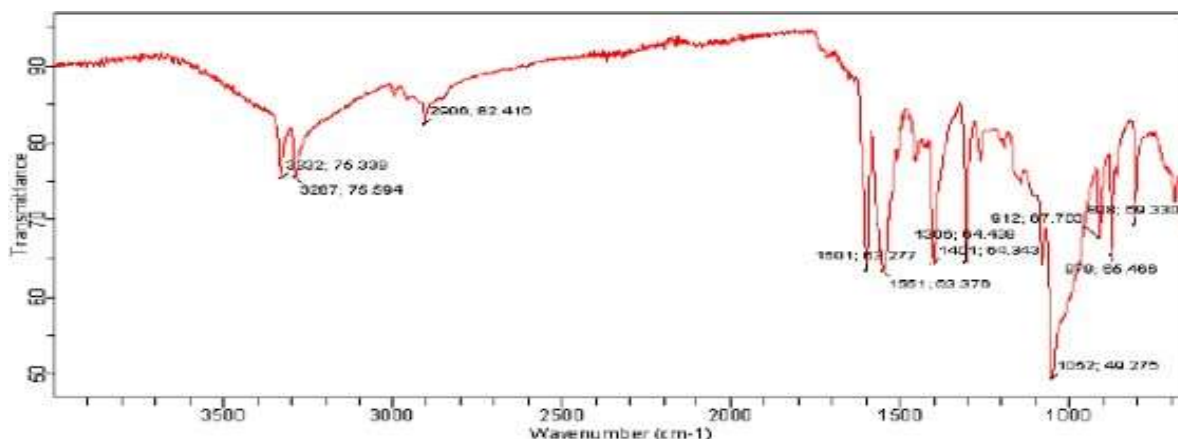


Fig. 7 FTIR analysis of CdS-Cysteine-Folic acid

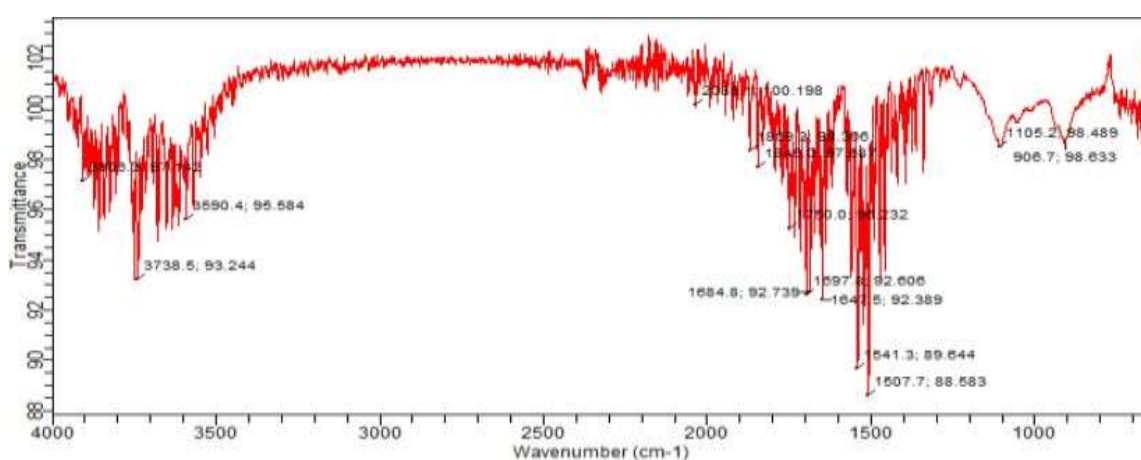


Fig. 8 FTIR analysis of CdS-Cysteine-Methotrexate-Folic acid

Scanning electron microscopy-energy dispersion spectroscopy (SEM-EDS)

For the detailed examination of the surface morphology to figure out the fundamental modification within a structure and to confirm the different bonding concomitant with MTX-CdS QDs nanoparticles SEM analysis was performed. SEM analysis of the powder verified that there were unique stipulations within the surface morphology of MTX-CdS QDs nanoparticles. The surface of the powdered sample was scanned on a magnification power of 2000X. The general surface of MTX-CdS QDs nanoparticles was in tightly packed confirmation and free from agglomeration. The particles were evenly spaced across the surface and provided details on the entire morphology. The SEM equipped with EDS provided the peak for confirmation of elemental analysis of MTX-CdS QDs NPs. SEM images demonstrated that NPs were free from the cluster and their composition elements like Cd and S were confirmed via EDAX analysis (Hewa-Rahinduwege *et al.*, 2021)

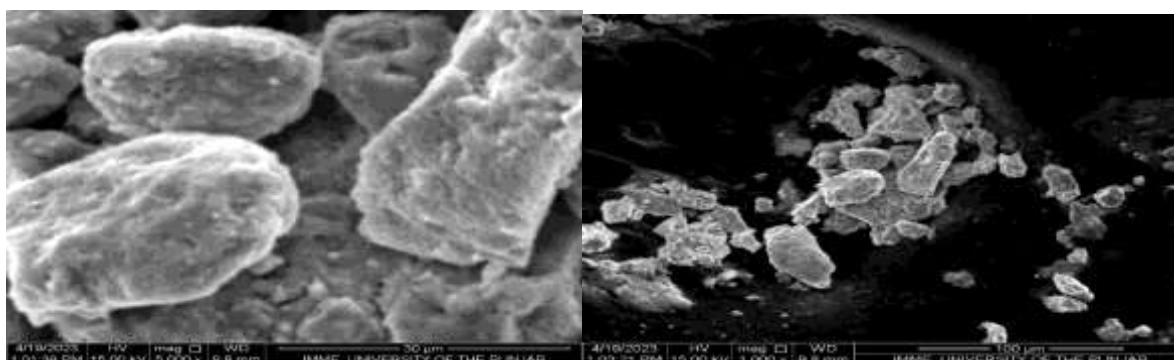


Fig. 9 Representative images of SEM-EDS of MTX-CdS QDs nanoparticles

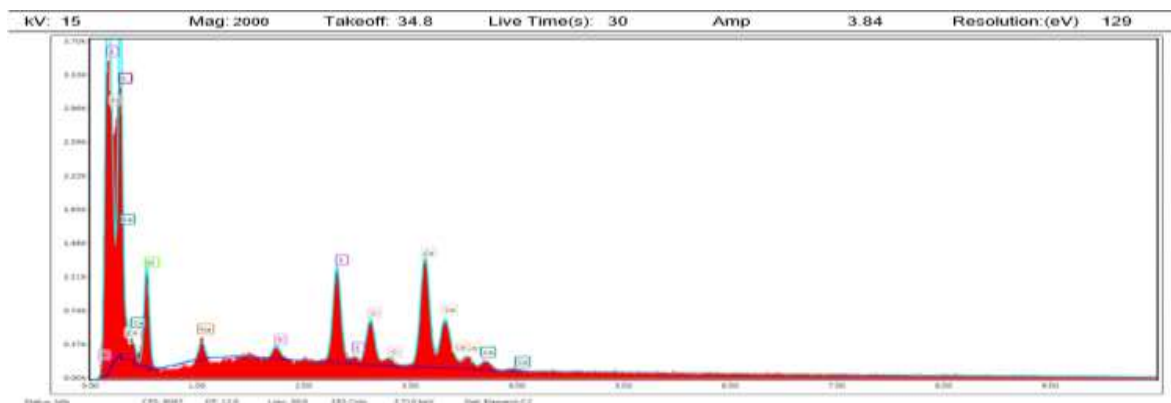


Fig. 10 Representative images of SEM-EDS of MTX-CdS QDs nanoparticles

X-ray diffraction analysis (XRD)

XRD was used to study the powder sample of MTX-CdS QDs for the analysis of their crystalline structure and size. According to the above mentioned figure which demonstrates the diffraction peaks for the MTX-CdS QDs, and the structure was discovered to be in a monoclinic system. On studying the XRD spectra of the MTX-CdS QDs, seven characteristic diffraction peaks were observed at 2θ values 32.92° , 47.19° , 55.89° , 58.71° , and 68.45° as per the finding of other researchers.

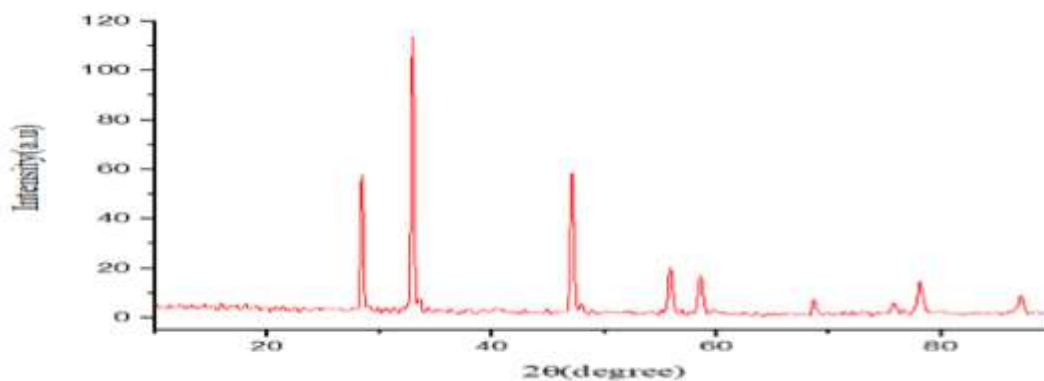


Fig. 11 XRD spectra of MTX-CdS QD

Table. 3 XRD pattern peaks for MTX-Cds QDs

Peak No.	Angle 2θ (degree)
1	32.92
2	47.19
3	55.89
4	58.71
5	68.45

For MTX-CdS QDs, the typical crystallite size ranges from 1 to 100 nm. Additionally, it is clearly shown that there were no contaminants other than peaks of cadmium acetate in the phase with high purity (Preethi & Philominal, 2022). It was confirmed that CdS QDs nanomaterials are formed and are crystalline. Since cadmium was able to make up a sizeable peak region in the doped sample, it is recognized that it successfully replaced the sodium positions without introducing any other flaws. The average size of the crystal was calculated via the Scherrer equation.

$$L = 0.9\lambda / (\beta \cos\theta)$$

L represents the size of the nanocrystal, λ is equal to the FWHM value, β is Bragg's diffraction angle, and θ is the wavelength of XRD radiations. The average size of MTX-CdS QDs from obtained diffraction peaks was 56nm. The doped QDs exhibited abridged intensity diffraction peaks, which indicated an increase in the crystal size due to doping.

Confirmation Test to Check the *In-Vitro* Anticancer Activity of MTX- CdS QD Nanocomposites on MCF-7 cells

Anticancer activity of MTX-CdS QDs nanocomposites checked by performing tissue immunohistochemistry and MTT assay.

Tissue immunohistochemistry

Under fluorescent microscope the positive binding of folic acid conjugated with MTX-CdS QDs nanocomposite to the folate receptors present on the surface of cells present in tissues. It indicates that the MTX-CdS QDs nanocomposite has attached to the fixed tissue sample. Immunohistochemistry results show that liver cancer cells surface receptor binds with CdS QDs nanocomposite. We ligated folic acid on the surface of MTX-CdS QDs nanocomposite which was used to bind with the folate receptors overexpressed on the cell membranes of hepatic tissue.

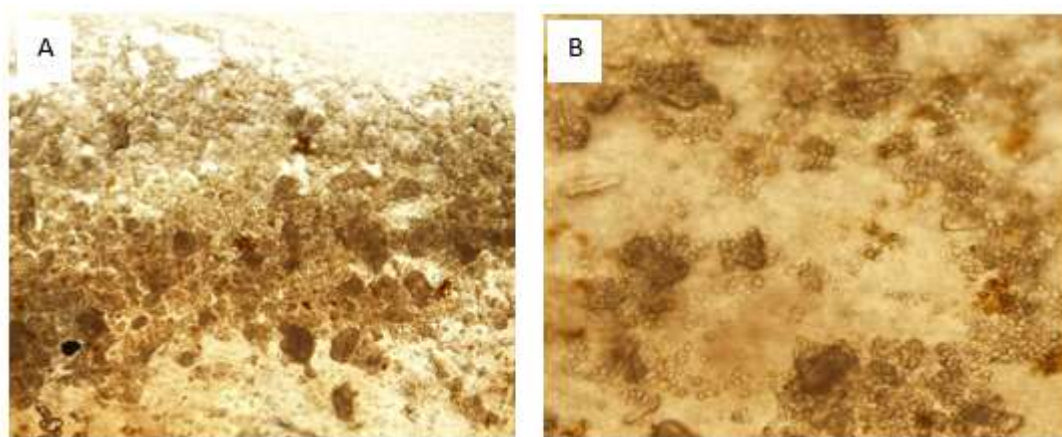


Fig. 12 Tissue immunohistochemistry (A) Control sample of liver cancer tissue in tissue immunohistochemistry. Liver cancer tissue sample having folate receptors on their cell surface (B) Test sample of liver cancer tissue in tissue immunohistochemistry. Binding of MTX-CdS QDs nanocomposite with liver cancer tissue sample through folate receptors

MTT Cell Viability Assay

MTT assay performed to check the viability of the cell. After addition of MTT reagent and detergent reagent in test sample and control sample a clear purple color was observed, this indicated that all the cells in control and test sample are viable. Mitochondria of viable cells produce an enzyme NADPH dependent oxidoreductase reduce MTT reagent (Tetrazolium dye) into formazan (purple color compound). In culture intensity of color indicates number of living cells.

Cell Death Rate in Test Samples in the Presence of MTX- CdS QD Nanocomposites There is clearly light color was observed in test samples as compared to control sample because cell death rate is high in the presence of MTX- QD nanocomposites because there were dead cells so less NADPH dependent oxidoreductase produced by mitochondria and intensity of purple color decreases in test sample
Viable Cells Present in Control Sample Viable MCF-7 cells were present in control sample after 72 hours of incubation with proper morphology

Dead MCF-7 Cells in Test Sample at Different Concentration of MTX- CdS QD Nanocomposites

At 100ng concentration of drug more cells started to lose their structure separated from each other but maintain their morphology more viable cells were present at low concentration of drug. At 200ng concentration of drug cells viability started to decrease and cells lose their proper Morphology. At 300ng concentration of drug cells viability decreased continuously. At 400ng concentration of drug more dead MCF-7 cells were present with no proper morphology. At 500ng concentration of drug only few viable MCF-7 cells were present after 72 hours of incubation with MTX-CdS QDs nanocomposite

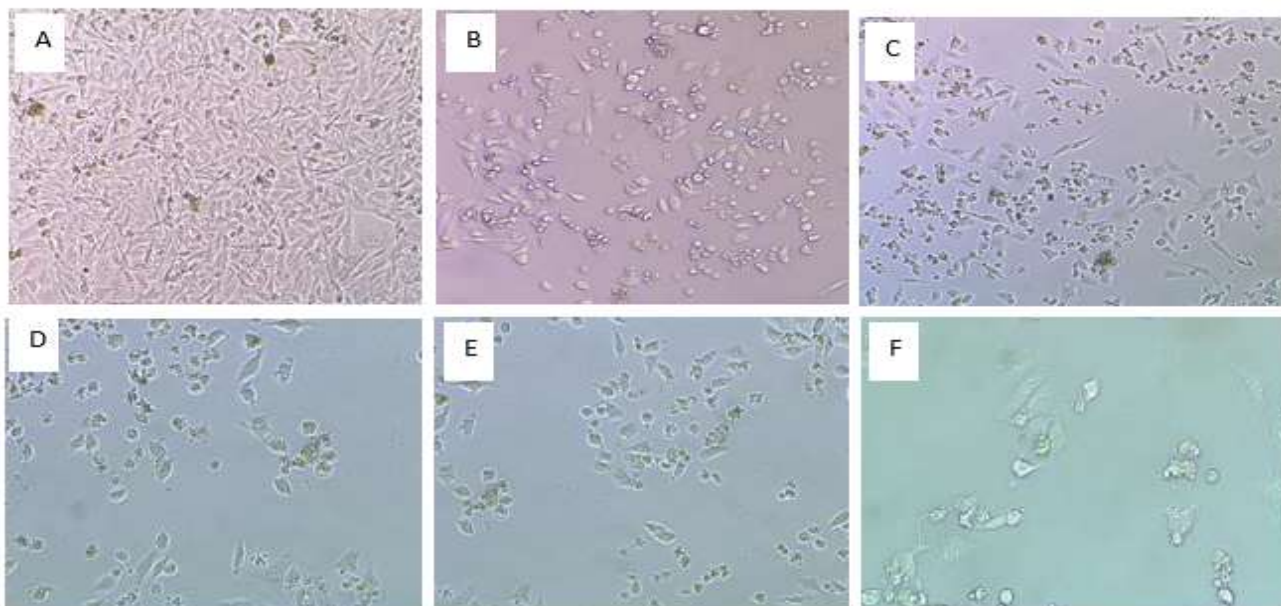


Fig.13 Dead MCF-7 Cells in Test Sample at Different Concentration of MTX- CdSQD

Nanocomposites (A) Viable cells present in control sample (B) Effect on MCF-7 cells at 100ng concentration of drug (C) Effect on MCF-7 cells at 200ng concentration of drug (D) Effect on MCF-7 cells at 300ng concentration of drug (E) Effect on MCF-7 cells at 400ng concentration of drug (F) Effect on MCF-7 cells at 500ng concentration of drug.

ELISA microplate reader Absorbance Analysis

ELISA microplate reader absorbance analysis interpret the effect of different MTX- CdS QDs nanocomposites concentration on the viability of MCF-7 cells at the wavelength of 570nm. Absorbance value decreased in test samples which shows the decrease in cell proliferation because there is decrease in NADP synthesis in cancer cells by adding MTX-QD nanocomposites which ultimately cause cell death while in control sample there is normal cell proliferation. MCF-7 cells show 21.87% viability and 78.13% cells death at 500ng concentration of MTX- CdS QDs nanocomposites Table 4

Table 4. 3. ELISA microplate reader absorbance analysis on MCF-7 cells viability with different MTX- CdS QDs nanocomposites concentration at the wavelength of 570nm.

Drug Concentration (ng /mL)	Absorbance	Cell Viability (%)
0	0.825	100
100	0.616	74.66
200	0.278	33.69
300	0.226	27.39
400	0.192	23.27
500	0.180	21.87

ELISA microplate reader Absorbance Analysis Graph

The absorbance value of control the viability of cells is 100% but as the concentration of drug increase cells viability decreases and cells show 21.87% viability and 78.13% cells death at 500ng concentration of MTX- CdS QDs nanocomposites

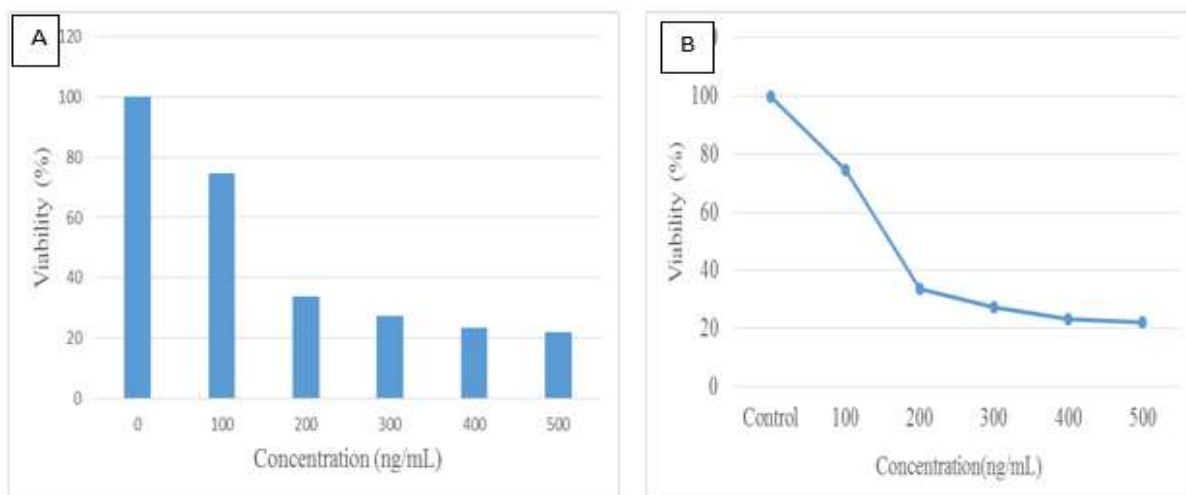


Figure 14 (A) ELISA microplate reader absorbance analysis on MCF-7 cells viability with different MTX- CdS QDs nanocomposites concentration at the wavelength of 570nm. (B) MCF-7 cells viability decreases as the concentration of MTX- CdS QDs nanocomposites was increases

CONCLUSION

In summary, we have successfully synthesized MTX-QD Nanocomposites for the treatment of cancer. Cancer is a multifactorial disease and the second major reason of deaths in the world. The major drawbacks of conventional therapies are drug targeting cause of cytotoxicity of healthy cells, bioavailability issues and require high amount of anticancer drug dose. So Quantum dots provide a platform in medical field assist in real-time tissue imaging and also cancer biomarker detection. The active targeting moieties on QD surface used to increase their gathering at tumor site and interactions with cancer cell-specific. CdS QDs functionalized with folic acid and methotrexate for drug delivery by targeting overexpressed folate receptors on surface of MCF-7 cells and destroy cancer cells. This strategy is cost effective and time saving in the formation of CdS QDs- MTX nanocomposites as compared to traditional cancer treatment methods. CdS QDs- MTX nanocomposite has less side effects to normal healthy cells, require low doses of anticancer drug with high efficacy which results in less toxicities to specific organ and also does not affect the activities of normal cell only target the cancer cell and release anticancer drug. CdS QDs- MTX nanocomposites can be used to cure autoimmune disorders and different types of cancer for example leukemia, non-Hodgkin's lymphoma, bladder cancer, bone cancer, breast cancer, head and neck cancer, stomach cancer, and choriocarcinoma with less side effects as compared to conventional cancer therapies.

REFERENCE

1. Bonacci, T., & Emanuele, M. J. (2020). Dissenting degradation: Deubiquitinases in cell cycle and cancer. *Seminars in Cancer Biology*, 67, 145–158. <https://doi.org/10.1016/j.semcan.2020.03.008>
2. Ganguly, A., & Nath, S. S. (2020). Mn-doped CdS quantum dots as sensitizers in solar cells. *Materials Science and Engineering: B*, 255(November 2017). <https://doi.org/10.1016/j.mseb.2020.114532>
3. Hassan, T., Huang, X., Zhou, C., Khan, M. S. G., & Saeed, S. (2021). Nanoparticles in Cancer Treatment: A Narrative Review. *Proceedings of the Pakistan Academy of Sciences: B. Life and Environmental Sciences*, 58(3), 1–18. [https://doi.org/10.53560/PPASB\(58-3\)664](https://doi.org/10.53560/PPASB(58-3)664)
4. Hossen, S., Hossain, M. K., Basher, M. K., Mia, M. N. H., Rahman, M. T., & Uddin, M. J. (2019).

- Smart nanocarrier-based drug delivery systems for cancer therapy and toxicity studies: A review. *Journal of Advanced Research*, 15, 1–18. <https://doi.org/10.1016/j.jare.2018.06.005>
5. Irshad, A., Sarwar, N., Sadia, H., Riaz, M., Sharif, S., Shahid, M., & Khan, J. A. (2020). Silver nano-particles: synthesis and characterization by using glucans extracted from *Pleurotus ostreatus*. *Applied Nanoscience (Switzerland)*, 10(8), 3205–3214. <https://doi.org/10.1007/s13204-019-01103-4>
 6. Kadam, V., Jagtap, C., Alshahrani, T., Khan, F., Khan, M. T., Ahmad, N., Al-Ahmed, A., & Pathan, H. (2021). Influence of CdS sensitization on the photovoltaic performance of CdS:TiO₂ solar cell. *Journal of Materials Science: Materials in Electronics*, 32(24), 28214–28222. <https://doi.org/10.1007/s10854-021-07198-2>
 7. Klochkov, S. G., Neganova, M. E., Nikolenko, V. N., Chen, K., Somasundaram, S. G., Kirkland, C. E., & Aliev, G. (2021). Implications of nanotechnology for the treatment of cancer: Recent advances. *Seminars in Cancer Biology*, 69, 190–199. <https://doi.org/10.1016/j.semcan.2019.08.028>
 8. Kumari, S., Sharma, N., & Sahi, S. V. (2021). Advances in cancer therapeutics: Conventional thermal therapy to nanotechnology-based photothermal therapy. *Pharmaceutics*, 13(8), 1174. <https://doi.org/10.3390/pharmaceutics13081174>
 9. Majeed, M. I., & Qaddoori, H. T. (2023). NANOTECHNOLOGY TARGETING DRUG DELIVERY WITH BIOSENSOR -A. *Academia Globe*, 3(03), 39–56. <https://doi.org/10.47134/academia.v3i3.852>
 10. Malik, S., & Muhammad, K. (2023). Nanotechnology : A Revolution in Modern Industry. *Molecules*, 28(2), 661.
 11. Meel, R. Van Der, Sulheim, E., Shi, Y., Kiessling, F., & Mulder, W. J. M. (2019). Smart cancer nanomedicine. *Nature Nanotechnology*, 14(11), 1007–1017. <https://doi.org/10.1038/s41565-019-0567-y>
 12. Omidian, H., Wilson, R. L., & Cubeddu, L. X. (2024). Quantum Dot Research in Breast Cancer : Challenges and Prospects. *Materials*, 17(9), 2152.
 13. Phafat, B., & Bhattacharya, S. (2023). Quantum Dots as Theranostic Agents : Recent Advancements , Surface Quantum Dots as Theranostic Agents : Recent Advancements , Surface Modifications , and Future Applications. *Mini Reviews in Medicinal Chemistry*, 23(12), 1257–1272. <https://doi.org/10.2174/138955752266622040520222>
 14. Raj, S., Khurana, S., Choudhari, R., Kesari, K. K., Kamal, M. A., Garg, N., Ruokolainen, J., Das, B. C., & Kumar, D. (2021). Specific targeting cancer cells with nanoparticles and drug delivery in cancer therapy. *Seminars in Cancer Biology*, 69, 166–177. <https://doi.org/10.1016/j.semcan.2019.11.002>
 15. Shamsi, U. (2020). Cancer Prevention and Control in Pakistan: Review of Cancer Epidemiology and Challenges. *Liaquat National Journal of Primary Care*, 2(1). <https://doi.org/10.37184/lnjpc.2707-3521.1.20>
 16. Sheth, V., Wang, L., Bhattacharya, R., Mukherjee, P., & Wilhelm, S. (2020). Strategies for Delivering Nanoparticles across Tumor Blood Vessels. *Advanced Functional Materials*, 31(8), 2007363. <https://doi.org/10.1002/adfm.202007363>
 18. Wang, S., Yu, J., Zhao, P., Li, J., & Han, S. (2021). Preparation and mechanism investigation of CdS quantum dots applied for copper ion rapid detection. *Journal of Alloys and Compounds*, 854, 157195.